

Magnetic and thermodynamic properties of $RMnO_3$ ($R = \text{Pr}, \text{Nd}$)

J. Hemberger¹, M. Brando¹, R. Wehn¹, V.Yu. Ivanov², A.A. Mukhin², A.M. Balbashov³, and A. Loidl¹

¹*Experimentalphysik V, Elektronische Korrelationen und Magnetismus,
Institut für Physik, Universität Augsburg, D-86135 Augsburg, Germany*

²*General Physics Institute of the Russian Academy of Sciences, 119991 Moscow, Russia*

³*Moscow Power Engineering Institute, 105835 Moscow, Russia*

The ground state properties of the pure perovskite compounds PrMnO_3 and NdMnO_3 were investigated by magnetization, magnetic AC susceptibility and specific heat measurements. A strongly anisotropic behavior has been detected for temperatures below the antiferromagnetic phase transition $T_N \approx 100$ K. The susceptibility and the weak spontaneous ferromagnetic moment appear to be different in both compounds due to different anisotropic rare earth contributions. The specific heat shows strong Schottky type contributions at low temperatures, which for NdMnO_3 strongly depend on the magnetic field. A spin reorientation phase transition (spin-flop type) induced by a magnetic field along b axis was observed in NdMnO_3 at $H \sim 110$ kOe and $T = 5$ K. All results can consistently be explained by anisotropic contributions of the rare earth ions: In PrMnO_3 the electronic ground state is determined by a low lying quasidoublet split by the crystal field (~ 19 K). In NdMnO_3 the Kramers doublet is split by an exchange Nd-Mn field (~ 20 K).

PACS numbers: 75.30.-m, 75.10.Dg, 77.30.Kg, 72.80.Ga

In recent years perovskite-type manganites have attracted considerable interest particularly due to the appearance of complex magnetic and transport properties, such as the colossal magneto resistance effect (CMR).¹ In these materials the physical properties are determined by a delicate interplay of charge, spin, orbital, and lattice degrees of freedom.² Substituting the A-site trivalent rare earth (R) by divalent Sr or Ca ($R_{1-x}A_x\text{MnO}_3$) changes the filling of the $3d$ Mn bands, introducing double-exchange interactions and thereby reducing Jahn-Teller type distortion and orbital order.³ In addition doping also changes the tolerance factor, which reflects deviations from the ideal perovskite structure.⁴ The Mn-O-Mn bond angle can be altered and the super-exchange between the Mn sites is influenced. As a result the perovskite manganites exhibit a rich phase diagram including different types of ordering phenomena and ground states like charge order, orbital order and antiferromagnetic (AFM) or ferromagnetic (FM) insulators or metals.⁴

Focusing on the parent compounds, the undoped manganites, the question arises, how, in addition to a small change in the tolerance factor, the specific choice of the R ion may alter the magnetic properties. Pure LaMnO_3 exhibits a Jahn-Teller distorted orthorhombic structure below $T \approx 800$ K and changes from an insulating paramagnet to an insulating antiferromagnet at $T_N \approx 140$ K.^{5,6} Substituting the nonmagnetic trivalent La by isovalent Pr or Nd, the electronic configuration of the Mn ions is qualitatively conserved and an orbitally ordered A-type AFM ground state is established.^{7,8,9} But how do the magnetic degrees of freedom of the Pr^{3+} and Nd^{3+} interact with the ordered Mn^{3+} sublattice and contribute to magnetic properties of the manganites? The purpose of this work is to shed some light on the role of the magnetic R ions and the mechanisms which determine the low temperature magnetic and thermodynamic properties in the pure perovskite manganites.

The single crystalline samples investigated in this work have been prepared by zone melting as described elsewhere.¹⁰ In contrast to LaMnO_3 which is rather sensitive to growth conditions and thermal processing parameters, PrMnO_3 and NdMnO_3 reveal a much weaker dependence of their properties on these parameters indicating a higher stoichiometric stability. X-ray diffraction pattern, taken at room temperature, revealed a single-phase orthorhombic Pbnm structure with the lattice constants $a = 5.448(6)$, $b = 5.822(6)$, $c = 7.582(0)$ for PrMnO_3 and $a = 5.415(9)$, $b = 5.837(9)$, $c = 7.548(1)$ for NdMnO_3 . These data are in very good agreement with the data of stoichiometric samples described in literature.¹¹ A comparison of our results to studies of the dependence of the lattice parameters in compounds with non-isovalent impurities or oxygen deficiency^{12,13,14} gives an upper limit of the defect of our samples of 0.5 %. Another evidence for the quality of our samples is the Neel temperature which for NdMnO_3 and PrMnO_3 refers to the highest cited in literature. It is known that T_N is significantly reduced upon the smallest deviations of the nominal stoichiometry.^{14,15}

Laue diffraction was utilized to orient the samples with respect to the pseudo-cubic crystallographic axis. The magnetization measurements were performed using a commercial SQUID system (MPMS, QUANTUMDESIGN) between 1.8 K and 400 K and in magnetic fields up to 50 kOe. Additional measurements were performed employing an extraction magnetometer and an AC susceptibility (OXFORD Teslatron) in fields up to 140 kOe. The specific heat has been measured on crystals with masses $m \lesssim 20$ mg at temperatures $5 \text{ K} \leq T \leq 250 \text{ K}$ with a noncommercial setup utilizing an AC method.

The temperature dependent measurements of the magnetic AC susceptibility are shown in Fig. 1. The AFM transitions show up as sharp peaks at $T_N = 99$ K for PrMnO_3 and $T_N = 88$ K for NdMnO_3 , respectively. For

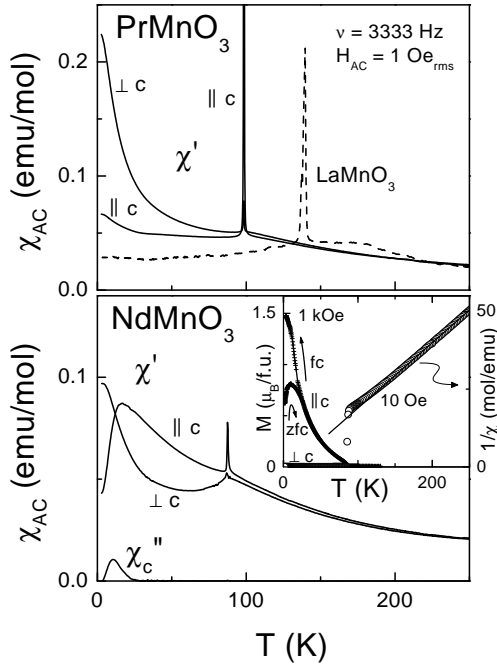


FIG. 1: Real part of the AC susceptibility χ'_{AC} of PrMnO_3 (upper frame) and NdMnO_3 (lower frame) measured along and perpendicular to the crystallographic c direction. The dashed line in the upper frame represents χ_{AC} of LaMnO_3 . For NdMnO_3 the imaginary part χ''_{AC} (loss) along c is shown as well. Inset: Reciprocal DC susceptibility (open circles, right scale) together with corresponding Curie-Weiss fit (straight line) and field-cooled/zero-field-cooled magnetization (crosses, left scale) of NdMnO_3 .

comparison the data as obtained in a twinned LaMnO_3 single crystal¹⁶ with $T_N = 139$ K are also shown (dashed line in the upper frame of Fig. 1). In the magnetically ordered regime of the R compounds a significant anisotropy shows up. The values of χ' in PrMnO_3 and NdMnO_3 are much higher than in LaMnO_3 , at least in the a, b plane. This obviously results from additional magnetic contributions of the R ions. At higher temperatures in the paramagnetic regime these contributions can easily be considered by adding the respective effective paramagnetic moment μ_{eff} . A Curie-Weiss fit to the susceptibility of NdMnO_3 , shown in the inset of Fig. 1, yields $\mu_{\text{eff}} = 6.16 \mu_B$ and $\Theta_{\text{CW}} \approx 10$ K. Experimental values for LaMnO_3 are $\mu_{\text{eff}} = 5.10 \mu_B$ and $\Theta_{\text{CW}} \approx 66$ K.¹⁶ The expected effective moment of $\mu_{\text{eff}} = 6.09 \mu_B$ for the superposition of the Nd ($4f^3$) and the Mn ($3d^4$) sublattice agrees well with the experimental findings. Similar results were obtained for PrMnO_3 .

To understand the enhanced anisotropic contributions below T_N one has to focus on the electronic ground state of the R ions, which via spin-orbit coupling depends on the local symmetry of the crystal field (CF) and on the exchange interaction with the Mn sublattice. The Pr compound reveals a strong increase of the susceptibility parallel to the a, b plane towards low temperatures.

Along the c direction χ remains almost constant, comparable to the behavior in LaMnO_3 . The AC susceptibility resembles the results reported from DC measurements.¹⁷ In NdMnO_3 the susceptibility of the a, b plane is slightly smaller than in PrMnO_3 , but below T_N and along c , χ' rises with decreasing temperature, reveals a cusp at $T \approx 18$ K and decreases towards lower temperatures. The drop off in the real part of the susceptibility of NdMnO_3 at about 10 K is accompanied by a peak in the imaginary part χ'' . In addition a distinct splitting between the DC magnetization measured under field-cooled (FC) and zero-field-cooled (ZFC) conditions can be detected below a splitting temperature $T_{\text{FC/ZFC}}$ as shown in the inset of Fig. 1. On increasing magnetic dc field the splitting is shifted from temperatures close to T_N down to $T_{\text{FC/ZFC}} \approx 22$ K for $H = 1$ kOe. This type of nonergodic behavior seems to be connected with the freezing of the domain dynamics within the ordered Mn sublattice. Nevertheless, the high values of the FC magnetization of up to $1.5 \mu_B/\text{f.u.}$ cannot be explained by the contribution of the Mn spins alone, because these are ordered in an A-type AFM structure, as discussed below. These phenomena, namely the FC/ZFC splitting and the loss features of the AC susceptibility, which appear only along the c direction, have rather to be interpreted in terms of domain freezing processes and the corresponding longitudinal relaxation of the Nd sublattice, polarized by the Nd-Mn exchange coupling.

High values of the FM component along c can also be detected in the hysteresis loops at $T = 5$ K, shown in Fig. 2. The lower frame of Fig. 2 shows the magnetization for NdMnO_3 up to 140 kOe. Along the c axis a spontaneous FM moment of $M_s \approx 1.7 \mu_B$ is detected. The corresponding value for PrMnO_3 , $M_s \approx 0.09 \mu_B$ (see inset of Fig. 2) is by a factor of ~ 20 smaller and comparable to the findings for LaMnO_3 .¹⁶ In PrMnO_3 and LaMnO_3 the small FM component arises from the canting of the A-type AFM structure due to Dzyaloshinsky-Moriya interaction, which is generated by a buckling of the orthorhombic oxygen octahedra.¹⁸ This explanation does not hold for the high values of M_s found in NdMnO_3 . A FM ground state of the Mn sublattice can be ruled out. Hole doping $R_{1-x}A_x^{2+}\text{MnO}_3$ leads to a FM ground state only for $x \gtrsim 0.1$.⁴ Also the jump in the magnetization at $H \approx 110$ kOe denotes a field induced spin-reorientation transition (spin-flop type).¹⁹ This effect can only be explained by the reorientation of the spins within an AFM spin structure. Thus the FM component along the c axis in NdMnO_3 has to be ascribed to the Nd spins. The Nd sublattice is polarized due to an effective exchange field of the Mn sublattice, which exhibits a small FM moment in c direction. At low temperatures the Nd spins are almost completely aligned in the internal exchange field, which is indicated by the drop of χ_c . In contrast the effective field due to the FM component of the Mn lattice in c direction does not couple to the Pr spins. In PrMnO_3 an enhanced susceptibility as well as a spontaneous magnetization along c are absent.

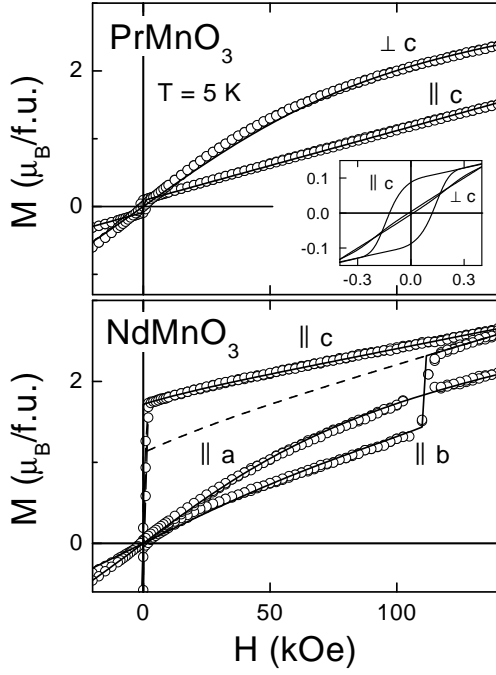


FIG. 2: Hysteresis loops of PrMnO_3 (upper frame) and NdMnO_3 (lower frame) measured for different orientations with respect to the magnetic field at $T = 5$ K. Lines denote fits employing the model described in the text.

To describe the observed experimental findings and to determine the ground state characteristics of the R ions one can utilize the models already used in the R orthoferrites having the same crystal structure, however G-type AFM ordering.²⁰ In RMnO_3 the ground multiplet of the R ions occupying low symmetry sites (point group C_s) is split by a CF into singlets for non-Kramers ions (Pr^{3+}) and into doublets for Kramers ions (Nd^{3+}). One arrives at an energy level scheme where the low-lying state is split due to crystal, external, and exchange fields. The exchange fields are determined by the isotropic and anisotropic R -Mn exchange, proportional to the FM and AFM vectors $\mathbf{F} = (\mathbf{M}_1 + \mathbf{M}_2)/2M_0$ and $\mathbf{A} = (\mathbf{M}_1 - \mathbf{M}_2)/2M_0$, respectively. There $\mathbf{M}_{1,2}$ denote the Mn sublattice magnetization of adjacent ferromagnetic layers with saturation value M_0 . For the Pr system the splitting of the quasidoublet (i.e. the two lowest CF split singlets) is of the form

$$\Delta^\pm \approx 2 \left[\Delta_{\text{cf}}^2 + (\Delta_z + \mu^\pm \mathbf{H})^2 \right]^{1/2}, \quad (1)$$

where $2\Delta_{\text{cf}}$ and $2\Delta_z = 2\Delta_z^0 A_z$ are the splittings by the CF and Pr-Mn exchange interactions²¹, and $\mu^\pm = (\mu_x, \pm\mu_y, 0)$ is the magnetic moment of the ground state which lies in the a, b plane. x, y, z correspond to a, b, c axis, respectively, and the signs \pm correspond to the two non-equivalent R positions. Here we have taken the observed magnetic anisotropy of the Pr contribution into account, namely the absence of a FM moment along the

c axis, implying that the moments of the Pr ions are oriented within the a, b plane.

Taking into account the local symmetry of the g-factor and the exchange field at the A-sites²⁰ the splitting of the Nd^{3+} Kramers doublet can be expressed through \mathbf{A} and \mathbf{H} by

$$\Delta^\pm \approx 2 \left[(\mu_z H_z + \Delta_y \pm \Delta_x)^2 + \Delta_z^2 + 2\mu'_y H_y \Delta_z + \mu_y^2 H_y^2 + \mu_x^2 H_x^2 \pm 2\mu_{xy}^2 H_x H_y \pm 2\mu'_x H_x \Delta_z \right]^{1/2}, \quad (2)$$

where $2\Delta_\alpha = 2\Delta_\alpha^0 A_\alpha$ (with $\alpha = x, y, z$) are the Nd-Mn exchange splittings and $\mu_{x,y,z,xy}$ and $\mu'_{x,y}$ are determined by the g-factor of the doublet and the Nd-Mn exchange parameters, respectively. Thus, in NdMnO_3 the splitting of the ground state is basically driven by the Nd-Mn exchange interaction, while in PrMnO_3 exchange splitting is absent in the $F_z A_y$ configuration, but instead the CF splitting dominates.

The magnetic properties were analyzed using the non-equilibrium thermodynamic potential

$$\Phi(\mathbf{H}, \mathbf{A}) = \Phi_{\text{Mn}}(\mathbf{H}, \mathbf{A}) - \frac{1}{2} N k_B T \sum_{i=\pm} \ln \left(2 \cosh \left(\frac{\Delta_i}{2k_B T} \right) \right),$$

where the corresponding potential of the Mn subsystem $\Phi_{\text{Mn}}(\mathbf{H}, \mathbf{A})$ was considered phenomenologically.¹⁸ The magnetization $\mathbf{M} = -\partial\Phi/\partial\mathbf{H}$ is defined by

$$M_x = \frac{2N\mu_x^2 H_x}{\Delta} \tanh \left(\frac{\Delta}{2k_B T} \right) + (\chi_\perp + \chi_x^{\text{VV}}) H_x$$

for $\mathbf{H} \parallel a$ and by

$$M_z = m_z^{\text{Mn}} + N\mu_z \tanh \left(\frac{\Delta}{2k_B T} \right) + (\chi_\parallel + \chi_z^{\text{VV}}) H_z$$

for $\mathbf{H} \parallel c$ with $\mu_z=0$ for PrMnO_3 . Here m_z^{Mn} is the weak ferromagnetic moment, χ_\perp the perpendicular susceptibility of the Mn subsystem, and $\chi_{x,z}^{\text{VV}}$ is the Van-Vleck susceptibility of the R ions due to excited states. In the case of the spin-flop transition along the b axis in NdMnO_3 the low and the high field regime have to be treated separately. The results of the simulation for the magnetization curves are shown as solid lines in Fig. 2 and the corresponding main parameters of the R ions are given in Tab. I and are in a good agreement with similar data evaluated recently from temperature dependent magnetization measurements¹⁷ and submillimeter optical studies.²³ A more detailed analysis of the spin reorientation and high-frequency magnetic excitations of NdMnO_3 will be presented in a separate publication.

To get an independent measure of the above determined values of the splitting Δ , we performed measurements of the specific heat in PrMnO_3 and NdMnO_3 in the temperature range from 5 to 250 K and in magnetic fields up to 50 kOe (see Fig. 3). The AFM transitions of both compounds show up as lambda-like anomalies

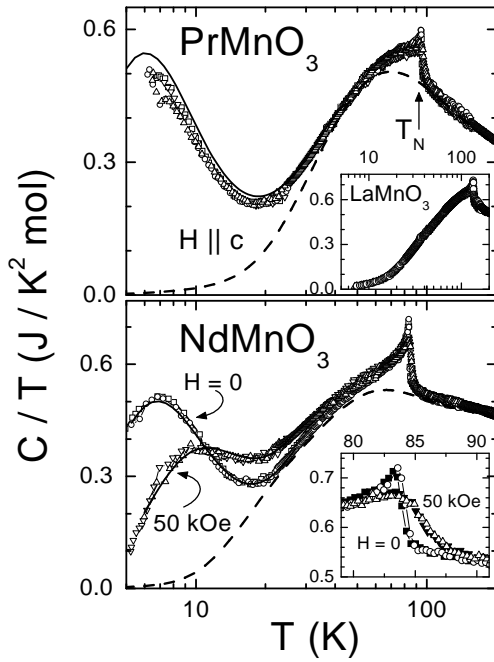


FIG. 3: Temperature dependence of the specific heat of PrMnO_3 (upper frame) and NdMnO_3 (lower frame) presented as C/T versus temperature on a logarithmic scale in external magnetic fields of 0 kOe (squares) and $H = 50$ kOe (triangles). The solid lines are calculated employing a two-level Schottky term as described in the text. Dashed lines display the lattice contribution. The inset in the upper frame shows the data for LaMnO_3 (non magnetic R). The inset of the lower frame displays the specific heat of NdMnO_3 near T_N .

which are smeared out in an external field (see the inset of the lower frame). A temperature hysteresis (open vs closed symbols) cannot be observed, neither at zero field nor at 50 kOe, indicative of a second-order transition. At low temperatures (below 20 K) in C/T a broad maximum appears in both, PrMnO_3 (upper frame of Fig.) and NdMnO_3 (lower frame). For comparison also the specific heat of LaMnO_3 was examined (see inset of the upper frame). Here this electronic contribution at low temperatures is absent.

Even if it is difficult to calculate and separate the specific heat of the lattice at elevated temperatures, we tried to parameterize the phonon contribution utilizing a Debye term ($\Theta_D \approx 285$ K) and two Einstein terms related to the minimal and maximal phonon energies in the perovskites.²² The results are shown as

dashed lines in Fig. . In addition a Schottky contribution for a two-level system (doublet) of the form $C \sim \Delta^2 / (T \cosh(\Delta/2k_B T))^2$ was used to fit the low temperature anomaly (solid lines in Fig. 3). The corresponding values for the splitting Δ are given in Tab. I. In zero external field the results are in excellent agreement with those obtained from the magnetization data. As given by Eq. (1) in the Pr system the splitting Δ is not changed by an magnetic field, while it is increased for NdMnO_3 . According to Eq. (2) one can estimate μ_c of the Nd ions from the difference between $\Delta(H_c=0)$ and $\Delta(H=50\text{kOe})$, which again meets the first result (see Tab. I). These results are in accordance with optical measurements in the submillimeter regime.²³

In conclusion, we presented measurements of the magnetic susceptibility, magnetization and the specific heat of NdMnO_3 and PrMnO_3 . The susceptibilities and the field dependent magnetic hysteresis loops reveal a strong anisotropy, which could be modelled in terms of R contributions. The ground state splitting of the Pr^{3+} ions turns out to be determined by the crystal field, while in NdMnO_3 the splitting is caused by an effective Nd-Mn exchange field. The ground state splitting of both compounds is of the order of $\Delta \approx 20$ K and could independently be determined by measurements of the specific heat. From these studies it follows that the influence of the R sublattice has to be considered as additional driving force of the puzzling ground state properties of perovskite manganites.

This work was supported by the Bundesministerium für Bildung und Forschung (BMBF) via VDI/EKM: 13N6917 and by Sonderforschungsbereich 484 (Augsburg), and by the RFBR (00-02-16500).

TABLE I: Parameters gained from the fitting of the magnetization data (Fig. 2) and the Schottky contributions to the specific heat (Fig. 3)

	Pr	Nd
$\Delta(H_c = 0)$ [K] from C_p	19.3 ± 1	21.6 ± 1
$\Delta(H_c = 0)$ [K] from M	18.7 ± 1	20.2 ± 1
$\Delta(H_c = 50 \text{ kOe})$ [K] from C_p	19.3 ± 1	32.5 ± 1
μ_c [μ_B] from C_p		1.6 ± 0.1
μ_c [μ_B] from M		1.9 ± 0.1
$\mu_{\perp c}$ [μ_B] from M	2.1 ± 0.1	(a) 1.8 ± 0.1
		(b) 1.2 ± 0.1

¹ R. von Helmolt, J. Wecker, B. Holzapfel, L. Schultz, K. Samwer, Phys. Rev. Lett. **71**, 2331 (1993); K. Chahara, T. Ohono, M. Kasai, Y. Kanke, Y. Kozono, Appl. Phys. Lett. **62**, 780 (1993).

² J. M. Coey, M. Viret, S. von Molnar, Adv. Phys. **48**, 167 (1999); E. L. Nagaev, Physics Reports **346**, 387 (2001);

M. B. Salomon, M. Jaime, Rev. Mod. Phys. **73**, 583 (2001).

³ M. Paraskevopoulos *et al.*, J. Magn. Magn. Mater. **211**, 118 (2000).

⁴ M. Imada *et al.*, Rev. Mod. Phys. **70**, 1039 (1998).

⁵ E.O.Wollan and W.C.Koehler, Phys.Rev. **100**, 545 (1955).

⁶ G.J. Jonker and J.H. Van Santen, Physica **16**, 337 (1950).

- ⁷ S.Y. Wu *et al.*, J. Appl. Phys. **87**, 5822 (2000).
- ⁸ A. Muñoz *et al.*, J. Phys.: Condens. Mat. **12**, 1361 (2000).
- ⁹ S. Quezel-Ambrunaz, Bull. Soc. Fr. Minéral. Cristallogr. **B 91**, 339 (1968).
- ¹⁰ A.M. Balbashov *et al.*, J. Cryst. Growth. **167**, 365 (1996).
- ¹¹ V.A. Cherepanov, L.Yu. Barkhatova, A.N. Petrov, and V.I. Voronin, J. Sol. State Chem. **118**, 53 (1995)
- ¹² K. Kitayama and T. Kanazaki, J. Sol. State Chem. **182**, 236 (2001).
- ¹³ N. Kamehashira and Y. Miyazaki, Mat. Res. Bull. **19**, 1201 (1984).
- ¹⁴ Z. Jiráček *et al.*, J. Appl. Phys. **81**, 5790 (1997).
- ¹⁵ C. Ritter *et al.*, Phys. Rev. B **56**, 8902 (1997).
- ¹⁶ M. Paraskevopoulos *et al.*, J. Phys.: Cond. Mat. **12**, 3993 (2000).
- ¹⁷ A.A. Mukhin *et al.*, J. Magn. Magn. Mater. **226-230**, 1139 (2001).
- ¹⁸ A. Pimenov *et al.*, Phys. Rev. B **62**, 5685 (2000).
- ¹⁹ Due to twins in a, b -plane with interchanged a and b axis the spin-flop transition in NdMnO_3 as observed for the two perpendicular directions in the a, b -plane at the same threshold field. Taking into account that only H is parallel to the b -axis could induce a spin-flop type transition from the magnetic ground state $F_z A_y$, we were able to extract pure magnetization along both a and b axis shown in Fig. 2 (lower frame).
- ²⁰ R.M. White, J. Appl. Phys. **40**, 1061 (1969); T. Yamaguchi and K. Tsushima, Phys. Rev. B **8**, 5187 (1973).
- ²¹ We assume here that the \mathbf{F} is eliminated by a standard minimization procedure and is expressed through dimensionless AFM moment \mathbf{A} .
- ²² F. Mayr *et al.*, Phys. Rev. B **62**, 15673 (2000).
- ²³ A.A. Mukhin *et al.*, Phys. Met. Metallogr. **91**, Suppl.1, 194 (2001).